### Not Macro, Not Micro, But Meso: Three Coarse-Grained Methods for Thermodynamic Properties of Partially Structured Fluids

J. M. Prausnitz
Chemical Engineering Department
University of California, Berkeley
and
Chemical Sciences Division
Lawrence Berkeley National Laboratory
Berkeley, CA 94720

#### **Abstract**

Macroscopic thermodynamics (e.g., classical equations of state) cannot provide an adequate description of the equilibrium properties of complex fluids or of simple fluids under near-microscopic constraints; such fluids have partial structure. Microscopic thermodynamics, through atomistic-level theory or simulations, can give such a description in principle but the required calculations are often excessive. Mesothermodynamics provides an intermediate method by describing fluids on a scale that reflects the fluid's significant (but not detailed) properties as determined by whatever is responsible for partial structure. Mesothermodynamics is not new but has made remarkable progress. To introduce its achievements to a wide audience, three examples are presented: phase transitions in a diblock copolymer; liquid-liquid equilibria in a binary mixture confined within a narrow pore; and pattern recognition by adsorption of a statisticallycharacterized heteropolymer on a statistically-characterized surface. Each example uses a somewhat different method: Landau expansion, density-functional theory and field theory. All three examples show that meso-thermodynamics can yield analytic results for the phase behavior of partially-structured fluids. Therefore, mesothermodynamics provides a powerful tool for development of new materials and for calculating thermodynamic properties of fluids under geometric constraints such as interfaces.

#### **Introduction**

The present situation in applied chemical thermodynamics suggests that we are now in a state of transition; the traditional, phenomenological era--we might call it the classical van der Waals era--has been exhausted and the likely future, provided by molecular simulation, is now only in its early stages.

Macrothermodynamics is characterized by semi-empirical equations of state or by a variety of crude models for condensed phases that reflect molecular properties in a more-or-less phenomenological manner. By contrast, microthermodynamics is a truly molecular science because it is based on the powerful scale-up method that we call statistical mechanics. Because analytical methods in statistical methods can be prohibitive, molecular simulation with large computers provides an increasingly popular alternative, limited primarily by not-yet-fast-enough computers.

Macrothermodynamics is now mature but far from dead; many practical problems in chemical (and related) technology can be solved or at least informed by conventional methods. While microthermodynamics is already useful for some applications, it is not yet sufficiently developed for most practical problems, especially those encountered in engineering. However, there can be little doubt that microthermodynamics is the wave of the future.

Mesothermodynamics provides an intermediate approach; the Greek word MESO means "middle". Mesothermodynamics abandons the bulk view. Instead, it looks at properties of materials using a scale that is larger than that used in microthermodynamics. In the microworld, the scale corresponds to atomic dimensions, perhaps a few Angstrom, while in the macroworld,

the scale is usually much larger, perhaps a million Angstrom. The scale in mesothermodynamics depends crucially on the problem of interest but, in general, it is somewhere between the extremes set by the micro and macroworlds.

Mesothermodynamics uses statistical mechanics and, with rare exceptions, is content to rely on analytic (as opposed to simulation) solutions of equations. It looks on molecular phenomena in a myopic way: the details are blurred but the significant characteristic structure is retained. Thus, mesothermodynamics is based on coarse-graining, a view that uses a semi-powerful microscope that can see the main, overall aspects of a molecular assembly but cannot see the fine features. Thus, a mesopicture of the United States would show all the major rivers and cities but would not provide every stream or brook and not every house and tree.

Mesothermodynamics is particularly useful for describing the properties of partiallystructured fluids, that is, those fluids where the scale of order in the arrangement of molecules
goes beyond atomic dimensions. Examples include liquid crystals, some kinds of emulsions,
domain-forming block copolymers and fluids confined by walls as in pores or at interfaces. Such
partially-structured fluids can be described by molecular simulation and in the future, it is likely
that simulation will be the method of choice. But, for partially-structured fluids, molecular
simulation gives more detail than we need and, with present computers, the required time for
simulation calculations may be prohibitive.

While mesothermodynamics is not new, in recent years, it has advanced remarkably. The purpose of this article is to provide a brief introduction to a wide audience, to show by examples how mesothermodynamics proceeds and what results can be achieved. In this brief introduction

all details have been omitted; its purpose is no more than to present the flavor of mesothermodynamics and to indicate its potential broad range of applicability. Toward that end, three examples from the literature are discussed below.

#### I - Domains in a Block-copolymer Melt. Application of the Landau Expansion

An early application of mesothermodynamics is directed at calculating the phase diagram of a block-copolymer whose sequence of segments A and B is not distributed in a random manner along the polymer chain; instead, segments A and B are distributed in blocks:

...AAAAABBBBBAAAAA... The simplest case is a diblock copolymer whose structure is indicated by ...AAAAAABBBBBBBB... In this example, per molecule, the number of A segments is equal to the number of B segments but, in general, that need not be. Let f = fraction of segments that are of type A. It follows that the fraction for B is 1-f.

At high temperatures, a diblock copolymer melt is a homogeneous phase because the entropic contribution to the Helmholtz energy of mixing is dominant, but at low temperatures, the positive enthalpy of mixing AAA... with BBB... may cause phase separation on a meso scale. In that event, the melt is no longer homogeneous. It is then a fluid consisting of adjacent A-rich and B-rich domains.

The mechanical, thermal, optical and electric properties of a block copolymer depend on its mesostructure. It is therefore of interest in applied materials science to establish that structure from fundamental properties of the polymer molecule.

For an incompressible fluid, at a fixed temperature, the overall (macroscopic) density  $\rho$  is constant. That density is the sum of two partial densities, one for A and one for B:

$$\rho = \rho_A + \rho_B \tag{1}$$

If domains are formed,  $\rho$  remains constant but  $\rho_A$  and  $\rho_B$  depend on position (designated by  $\vec{r}$ ). Equation (1) should therefore be rewritten

$$\rho = \rho_{A}(\vec{r}) + \rho_{B}(\vec{r}) \tag{1a}$$

In an A-rich domain,  $\rho_A$  is large while  $\rho_B$  is small; and vice-versa in a B-rich domain.

To establish the phase diagram, we define an order parameter  $\psi(\vec{r})$ 

$$\psi(\vec{r}) = f \rho_B(\vec{r}) - (1-f) \rho_A(\vec{r}) \tag{2}$$

For a disordered (completely mixed) system,  $\psi(\vec{r}) = 0$ .

When a domain is formed, it can have any one of a variety of geometric structures. The simplest, shown in Figure 1, is a laminar structure. For that structure, when  $f_A = f_B$ , the order parameter is of the form

$$\psi(\mathbf{r}) = \Delta \cos \mathbf{Q}\mathbf{r} \tag{3}\dagger \dagger$$

where frequency Q determines the lamellar thickness. For the disordered phase,  $\Delta = 0$ . If lamellae form,  $\Delta \neq 0$ .

To characterize interactions between A and B, we use conventional Flory parameter  $\chi$ 

$$\chi = \frac{2\epsilon_{AB} - (\epsilon_{AA} + \epsilon_{BB})}{kT} \tag{4}$$

where  $\epsilon_{ij}$  is the characteristic potential energy between (non-bonded) adjacent segments i and j;

<sup>†</sup>The word "parameter" is misleading because  $\psi(r)$  is a function, not a parameter. Regrettably, the words order parameter (instead of order function) are used pervasively in the literature.

<sup>††</sup>When  $f_A \neq f_B$  or when the Kuhn lengths for A and for B are not equal, additional terms must be added to Eq. (3). In general, Eq. (3) is a Fourier series.

Boltzmann's constant is designated by k and T is absolute temperature. It is important to note that  $\chi$  depends on temperature. When the numerator in Eq. (4) is independent of temperature (for nonpolar A and B),  $\chi$  is an inverse measure of T.

Q can be obtained from f,  $\chi$  and N (the total number of segments per molecule), and from Kuhn lengths  $l_A$  and  $l_B$ . (The Kuhn length is the statistical length of a segment similar to the persistence length: essentially, in a chain, it is the length of a segment that forms a straight line until there is a kink in the chain. Kuhn length provides an inverse measure of chain flexibility.)

But how do we find  $\Delta$ ? We do so by expanding the Helmholtz energy per unit volume A/V, in a Landau expansion:

$$\frac{A}{V} = 2N(\chi_s - \chi)\Delta^2 + K_3\Delta^3 + K_4\Delta^4 \dots$$
 (5)

Equation (5) is an expansion about A/V for the disordered system (where  $\Delta=0$ ). Here  $\chi_S$  is Flory's parameter evaluated at spinodal temperature  $T_s$ ; the spinodal temperature is the lowest temperature where the disordered phase is intrinsically stable. At  $T < T_s$ , there <u>must</u> be phase separation. At  $T > T_s$ , there <u>may</u> be (metastable) phase separation. The important quantity  $\chi_s$  depends on f; it is calculated from knowing N, f,  $l_A$  and  $l_B$ .

For a fixed temperature, A/V is minimized with respect to  $\Delta$  by functional differentiation of A/V with respect to order parameter  $\psi(r)$  given by Equation (3).

When A/V is at its minimum, the results are

For 
$$\chi < \chi_s$$
,  $\Delta = 0$  (6)

and there are no domains; the melt is homogeneous.

For 
$$\chi > \chi_s$$
,  $\Delta > 0$  and  $K_3 = 0$  (7)

$$\Delta = \mathcal{I}[N, K_4, (\chi - \chi_s)] \tag{7a}$$

Details in function  $\mathcal{F}$  are determined by whatever simplifying assumptions are made in the calculation of  $K_4$ . Because  $\chi \sim 1/T$ , Eqs. (6) and (7a) tell us first, that at high temperatures, there are no domains; second, because  $\chi_s$  is a known function of f, they provide the transition temperature as a function of f; and third, at low temperatures, Eqs. (1a), (2) and (3) give the local density profile, i.e., the variation of partial densities  $\rho_A$  and  $\rho_B$  in space.

Geometric structures other than lamellae can be postulated. For any assumed structure, it is necessary to write a suitable form of the density profile, similar to the simple lamellar case in Equation (3). For fixed conditions, the "true" structure is the one that gives the lowest Helmholtz energy.

Figure 2 shows two phase diagrams. The first one, now 17 years old, considers the symmetric case where the Kuhn length for A is the same as that for B. The product  $\chi N$  is plotted as a function of f;  $\chi N$  provides an inverse measure of temperature. Thus the bottom part of the phase diagram shows the high-temperature region where the copolymer is disordered. The upper part shows various ordered phases.

The second phase diagram considers an asymmetric diblock copolymer where the Kuhn length of A is larger than that of B. While only part of the phase diagram (0.45< $f_A$ <0.75) is shown, it is evident that the general features for the asymmetric case are similar to those for the symmetric case although various details are not. Both diagrams indicate that even for a simple diblock copolymer, a variety of geometric structures can appear, depending on conditions. Further, as expected, the diagrams show that at constant  $\chi$ , as N increases, formation of domains

becomes increasingly likely.

Finally, Figure 3 shows some recent experimental results for diblock polyisoprene-polystyrene. Again,  $N\chi$  is plotted against polymer composition ( $f_{IP}$  = fraction of isoprene). The parabola showing the transition from order to disorder is calculated.

With numerous refinements in the calculations, it is now possible to obtain nearly quantitative agreement between theory and experiment for simple cases. For complex phase diagrams like that in Figure 3, only semiquantitative agreement can now be achieved but, because further improvements appear regularly in the literature, more reliable calculations can be expected.

The key quantity discussed here is the density profile in a diblock copolymer. This profile does not give a detailed microscopic description; instead, it provides a coarse-grained picture of how a macroscopic quantity (density) varies in space that is measured in units comparable to those that characterize the polymer chain. This particular application uses mesothermodynamics to provide structural information for a heterogeneous material where the scale of heterogeneity is of the order of 100 or 1000 Å.

The next section is also concerned with calculation of density profiles. However, in that section attention is directed at a fluid mixture of ordinary (simple) molecules where partial order in the fluid is due not to inherent properties of the molecules but due to an outside restraint. In this case the characteristic scale is smaller, in the vicinity of 10 Å.

#### Phase Behavior of a Simple Liquid Mixture in a Narrow Pore

In nature, fluids are often in contact with porous solids. For example, water is in contact with the porous matter in plants; oil and natural gas are in contact with porous inorganic matter

under the ground. When the diameter of the pore is at most one order of magnitude larger than that of the molecule, we expect the properties of the confined fluid to be significantly different from those of the free fluid. By analogy, standing in a tiny filled-up elevator is different from standing on New York's Times Square on New Year's Eve. The densities are comparable but the exercisable degrees of freedom are not.

This illustration of mesothermodynamics considers the application of density-functional theory toward calculation of phase behavior of a fluid confined to a narrow pore, as indicated in Figure 4.

Because the fluid in the pore is in equilibrium with the fluid outside the pore, the fluid's chemical potential  $\mu$  is constant, independent of the extent of confinement as measured (inversely) by H\*, the ratio of pore diameter H to molecular diameter  $\sigma$ . For a system at constant  $\mu$ , the most useful ensemble is that corresponding to grand partition function  $\Xi$ . The grand potential  $\Omega$  is related to  $\Xi$  by

$$\Omega = -kT \ln \Xi$$
 (1)

Let  $\rho$  stand for the density of fluid molecules in the pore. For short distances from the wall,  $\rho$  depends strongly on distance r where r goes from zero to H. To determine the properties of the confined fluid we need density profile  $\rho(r)$ .

Because  $\Omega$  depends on  $\rho(r)$ ,  $\Omega$  is a functional. The desired density profile is obtained by minimizing  $\Omega$  with respect to the density profile:

$$\frac{\delta\Omega[\rho(\mathbf{r})]}{\delta\rho(\mathbf{r})} = 0 \tag{2}$$

Upon applying a Legendre transformation, this minimization is equivalent to solving the

equation

$$\frac{\delta A[\rho(r)]}{\delta \rho(r)} = \mu - v(r) \tag{3}$$

where A is the Helmholtz energy and v(r) is the restraining potential imposed on the confined fluid, i.e., the potential due to the pore's walls.

Density-functional theory is used to find the density profile that satisfies Equation (2) or, equivalently, Equation (3).

A particular application of these ideas concerns a bulk binary fluid mixture in contact with a porous material where the pore width is H. In this fluid mixture, intermolecular forces are described by the Lennard-Jones potential; collision diameter  $\sigma_1$  (for component 1) is equal to  $\sigma_2$  (for component 2). Characteristic potential energy parameter  $\varepsilon_{11}$  is equal to  $\varepsilon_{22}$  but the energetic parameter for the unlike 1-2 pair  $\varepsilon_{12}=0.75$   $\varepsilon$  where  $\varepsilon$  is either  $\varepsilon_{11}$  or  $\varepsilon_{22}$ . For reduced temperatures (T\* = KT/ $\varepsilon$ ) less than about 0.91, this bulk-fluid mixture has only partial miscibility as indicated by the top line in Figure 7. The interaction of a wall molecule (w) with a fluid molecule is also described by a Lennard-Jones potential with  $\frac{\varepsilon_w}{k}$ =153 K and  $\sigma_w$  = 3.727 Å. The reduced number density of the wall is  $\rho_w \sigma_w^3 = 0.988$ . Density-functional theory gives analytic results for the total density profile in the pore; the composition profile in the pore; and, most interesting, the liquid-liquid coexistence curve as a function of reduced pore size H\*.

Figure 5 shows total density profiles for a slit pore of width  $H^* = 6$ . A slit pore is the space between two parallel walls. Coordinate r is perpendicular to the walls; it starts at one wall (r = 0) and ends at the other  $(r = 6\sigma)$ . The fluid mixture in the pore is in equilibrium with bulk fluid in the partial-miscibility region. Results are given for two temperatures; while the shape of

the profile is the same for both temperatures; the peaks and valleys of the profile are more pronounced (sharper) at the lower temperature. Results from density-functional theory are in excellent agreement with Monte-Carlo simulations.

Figure 6 shows composition profiles for three temperatures (mole fraction versus slit-pore coordinate r); each temperature corresponds to a particular bulk composition indicated by the horizontal lines labeled I, II and III. Results from density-functional theory are now in fair (but not perfect) agreement with those from Monte-Carlo simulation. The composition in the center of the pore is reasonably close to that in the bulk, but near the wall, the composition is significantly different from that in the bulk. This effect may be of particular interest in design of heterogeneous catalytic chemical reactors where the catalyst is supported by a porous material.

For thermodynamicists, the most interesting result is the liquid-liquid phase diagram shown in Figure 7. The outer dotted line gives the coexistence curve in the bulk ( $H^* = \infty$ ). The inner line gives the coexistence curve in the pore (with  $H^* = 6$ ) obtained from density-functional theory; the black and white points give results from Monte-Carlo simulation. (In the Monte-Carlo calculations, the white points follow from a sample box somewhat larger than that used for the black points.) While agreement is only fair, the important conclusion is supported by both kinds of calculation: the upper critical solution temperature in the pore lies below that in the bulk. In other words, for the particular conditions chosen here, the wall increases compatibility for components 1 and 2. At a reduced temperature of say, 0.90, the bulk fluid consists of two liquid phases but the confined fluid, in equilibrium with the bulk fluid, consists of only one liquid phase.

In some respects, this example of mesothermodynamics is similar to that for a block copolymer because both show how a macroscopic property (density) changes with position. However, in this second example the characteristic linear scale is now much smaller. While Monte-Carlo simulations were obtained to check the results, the method briefly outlined here, (density-functional theory), is analytic. While the situation may change, at present, calculations using density-functional theory are much faster than those using simulations, especially if results are desired for a variety of conditions.

Adsorption of Heteropolymers on a Heterosurface: Field Theory with Statistical Characterization

A new application of mesothermodynamics is provided by a framework for calculating adsorption of a statistically characterized polymer on a statistically characterized surface. For our purposes here, a heteropolymer is a chain molecule with at least 2 different monomers, say A and B. The statistical characterization of the heteropolymer concerns the sequence; at one extreme, (if the number of A monomers is equal to the number of B monomers), we may have a perfectly alternating sequence (ABABAB ...) while at the other extreme, we may have perfect segregation (...AAAABBB...). Similarly, a surface may have two (or more) types of sites; each type may have a preference for A or B. These sites can be distributed on the surface in a variety of ways; for example, the sites may be arranged at random or, they may be arranged in some pattern where sites of one type tend to be close together in a set of patches while sites of the second type are also close together in another set of patches. Adsorption of heteropolymers on surfaces depends not only on the energetics between monomers, and on energetics between monomers and surface sites, but also on the statistics of spatial arrangement that characterize the heteropolymer and the

heterosurface. Understanding such adsorption is useful not only for the design of lubricants and a variety of coatings for optical and electronic materials but also for design of pharmaceutical and diagnostic products.

The statistics of a bi-functional heteropolymer are given by two parameters,  $f_A$  and  $\lambda$  In a chain, the fraction of A monomers is given by  $f_A$ .

The sequence distribution of monomers A and B is given by  $\lambda$  defined as

$$\lambda = p_{AA} + p_{BB} - 1 \tag{1}$$

where

 $p_{AA}$  = probability that the segment following A is also A

 $p_{BB}$  = probability that the segment following B is also B

λ → 1 corresponds to a block copolymer ...AAABBBB...

 $\lambda = 0$  corresponds to a totally random copolymer

 $\lambda = -1$  corresponds to a perfectly alternating copolymer

...ABABABAB...

Consider an isolated chain with N connected monomers. To describe a polymer chain microscopically, it is necessary to specify the position  $\vec{r}$  of every connected monomer in the chain. In mesothermodynamics, i.e., in coarse-graining, the sequence of connected monomers is replaced by a continuous variable n. Function  $\vec{r}$  (n) gives the shape of the chain.

The Hamiltonian H of the chain is

$$\frac{H}{kT} = \frac{3}{21} \int_{0}^{N} d\mathbf{n} \left(\frac{d\mathbf{r}}{d\mathbf{n}}\right)^{2} + \frac{1}{2} \int_{0}^{N} \int_{0}^{N} d\mathbf{n} d\mathbf{n}' \, \phi \left[\mathbf{r}(\mathbf{n}) - \mathbf{r}(\mathbf{n}')\right] \tag{2}$$

where I is the average Kuhn length of the polymer chain. The first term corresponds to the elasticity entropy of the connected monomers according to the well-known bead-spring model for polymer chains. The second term gives a summation of the potential energy  $\phi$  between a monomer at n and another at n'. Hamiltonian H depends on  $\lambda$ .

The partition function Z is

$$Z = \iint D_{\mathbf{r}(\mathbf{n})}^{+} \exp -\frac{\mathbf{H}}{\mathbf{k}\mathbf{T}}$$
 (3)

where  $\int D \dot{r}$  (n) indicates summation over all possible shapes of the chain.

Equation (3) is for one chain. For an assembly of chains, additional integrals are defined. For the interaction between an assembly of chains with a surface, the integrals include also interactions between the chains and the surface. From the corresponding partition function it is then possible to calculate how the concentration of polymer changes with distance perpendicular to the surface. If the concentration near the surface exceeds the bulk concentration we have adsorption; if the concentration near the surface is below that of the bulk, we have depletion.

The integrals are complex but with some mathematical simplifications, they can be evaluated analytically. The necessary mathematical procedures are similar to those used by physicists in quantum electrodynamics (Feynman integrals). Because the theory of quantum electrodynamics is a field theory, the procedure for materials briefly indicated here is also called a field theory.

To characterize interaction of the heteropolymer with a homogeneous surface S, we define two parameters,  $\eta_B$  and  $\tau.$ 

Selectivity 
$$\eta_{\rm B} = \frac{\epsilon_{\rm AS} - \epsilon_{\rm BS}}{kT}$$
 (4)

If  $\eta_B = 0$  surface has no preference for A or B

 $\eta_B > 0$  surface prefers B

 $\eta_B < 0$  surface prefers A

Here  $-\epsilon_{AS}$  is the characteristic potential energy between monomer A and a surface site S; a similar definition holds for  $-\epsilon_{BS}$ .

The average characteristic potential energy for copolymer AB and surface S is given by  $\tau$ :

$$\tau = \frac{\epsilon_{AS} + \epsilon_{BS}}{2kT} \tag{5}$$

Figure 8 shows adsorption equilibria for a semi-concentrated solution of a totally random copolymer AB ( $\lambda=0$ ) on a homogeneous surface. Three plots are given; each one shows, for a fixed  $\tau$ , adsorption or depletion as a function of  $\eta_B$  and  $f_A$ . Figure 8 shows that, for a totally random copolymer AB, adsorption equilibria are a complex function of  $f_A$ ,  $\tau$  and  $\eta_B$ . In Figure 8,  $\lambda=0$ . For other values of  $\lambda$ , different adsorption equilibria are obtained.

In the first panel ( $\tau$  = -0.3), the average energy between surface and heteropolymer is attractive and therefore, when there is no selectivity ( $\eta_B$  = 0), adsorption occurs for all  $f_A$ . However, when  $f_A$  is small (i.e., the heteropolymer has mostly B monomers), we see depletion when the selectivity  $\eta_B$  is appreciably negative (lower left corner). When the selectivity  $\eta_B$  is appreciably positive, depletion again occurs when  $f_A$  is close to unity because the polymer then contains mostly A monomers (upper left corner); if  $\eta_B$  is positive, selectivity for A is necessarily negative; in other words, the surface does not like A. Similar qualitative interpretations hold for the third panel where  $\tau$  is positive. The middle panel ( $\tau$  = 0) shows a transition between the phase behaviors of the two outside panels with a critical point at zero selectivity and  $f = \frac{1}{2}$ .

To illustrate adsorption on a heterogeneous surface, Figure 9 considers two types of AB chains and two types of heterogeneous surfaces. The top chain represents a perfectly alternating copolymer (with  $f_A = \frac{1}{2}$ ) while the second chain represents a copolymer that is blocky.

The surface has two kinds of sites, • and o. The two surfaces shown in Figure 9 have equal densities of surface sites • and o but the distributions of these sites are not the same; one distribution (striated) has a "chessboard" shape and the other (patchy) has a "pancake" shape.

Quantitative description of these site distributions is achieved by assigning suitable radial distribution functions for sites • and o on the surface. Site• attracts A but repels B while site o attracts B and repels A.

Figure 10 shows calculated adsorption results for a dilute polymer solution; the probability of adsorption P is plotted against  $\sigma$ , the total density of sites on the surface. Four cases are shown: in the top diagram, results are for two types of heteropolymer on a statistically patchy surface while the one below gives results for the same two types of heteropolymer on a statistically striated surface. All four cases show discontinuities. These discontinuities indicate recognition; when adsorption suddenly increases, the surface has "recognized" the heteropolymer. The interesting feature of Figure 10 is that when  $\sigma$  is low, the statistically patchy surface selectively recognizes the statistically blocky heteropolymer, while the statistically striated surface selectively recognizes the statistically alternating heteropolymer.

The illustrative results shown in Figure 10 indicate that highly selective adsorption is possible when the statistics of adsorbate are matched with the statistics of the adsorbent.

The calculations briefly outlined here have been semi-quantitatively verified by two very

recent experimental studies in biotechnology. Arnold and co-workers at California Institute of Technology have shown that, by functionalizing a hydrophobic polymeric support with copper ions, it was possible to conduct a chromatographic separation that is highly specific to horse cytochrome-c. In other words, the functionalized support "recognizes" enzyme horse cytochrome-c selectively (while not "recognizing" other enzymes) because the distribution statistics of the functionalized surface match the distribution statistics (positive and negative charges) of that particular enzyme.

At Harvard, Whitesides and co-workers have studied the possibility of inhibiting viral attachment to cells by pre-adsorbing a polymer to the surface of the virus. When Whitesides studied adsorption of various heteropolymers to inhibit the influenza virus from attaching to mammalian erythrocytes, he found that for fixed  $\lambda$ , there is a particular range of f that leads to optimal viral inhibition.

#### Conclusion

The three examples presented here illustrate the goal of mesothermodynamics: to use analytic statistical mechanics for describing properties of materials whose molecules are assembled with a degree of order beyond that corresponding to atomic dimensions. Mesothermodynamics seeks to provide structural properties of interesting new materials or of conventional materials under some external geometric restraint. The examples are not discussed in detail; anyone who wants to do mesothermodynamic calculations must consult the original literature. The purpose here is only to provide an introduction, to give a glimpse of what mesothermodynamics is, how it proceeds and what kind of results may be achieved.

At this time in the world's technological history, there is increasing emphasis on new materials and on materials at interfaces. New materials tend to be those with intermediate-range structure and materials near interfaces are interesting precisely because they necessarily assume structures that are different from those in the bulk. Mesothermodynamics provides a powerful tool for calculating the properties of such materials. While molecular simulation may one day make mesothermodynamics obsolete, that day may be many years in the indefinite future. It is therefore likely that new developments in mesothermodynamics will continue and that they will find an ever-increasing variety of applications.

#### **Acknowledgment**

The author is grateful to J. Z. Wu, L. Lue, D. Bratko and A. Chakraborty for patient tutoring and advice. For financial support, the author is grateful to the Director, Office of Basic Energy Sciences, US Dept. of Energy, to the National Science Foundation, and to the Donors of the Petroleum Research Fund administered by the American Chemical Society.

### References

#### First Example

Edwards, S.F., Proc. Phys. Soc. (London) 88 265 (1966).

Leibler, L., Macromolecules 13 1602 (1980).

Matsen, M.W. and M. Schick, Phys. Rev. Lett. <u>72</u> 2660 (1994); Macromolecules <u>27</u> 4014 (1994). Fredrickson, G. and Helfand, E., J. Chem. Phys. <u>87</u> 697 (1987)

Khandpur, A.K., Forster, S., Bates, F.S., Hamley, I.W., Ryan, A.J., Bras, W., Almdal, K. and Mortensen, K., Macromolecules <u>28</u> 8796 (1995).

Goldenfeld, N., "Lectures on Phase Transitions and the Renormalized Group", Addison-Wesley (1992).

Bates, F.S. and Fredrickson, G.H., "Block Copolymer Thermodynamics - Theory and Experiment", Annual review of Physical Chemistry 41 525 (1990).

### Second Example

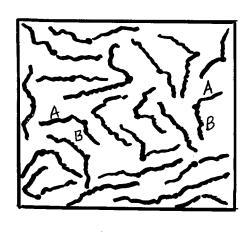
Kierlik, E., Fan, Y., Monson, P.A., and Rosenberg, M.L., J. Chem. Phys. <u>102</u> 3712 (1995). Kierlik, E. and Rosenberg, M.L., Phys. Rev. A <u>42</u> 3382 (1990). Evans, R., Density Functional in the Theory of Nonuniform Fluids, in "Fundamentals of Inhomogeneous Fluids" edited by Henderson, D., Marcel Dekker, Inc. (1992).

### Third Example

Gutman, L. and Chakraborty, A.K., J. Chem. Phys. 105 7842 (1996). Chakraborty, A.K., Tirrell, M., MRS Bulletin 21 28 (1996). Bratko, D., Chakraborty, A.K., and Shakhnovich, E.I., Phys. Rev. Lett. (76) 1844 (1996). Srebnik, S., Chakraborty, A.K. and Shakhnovich, E.I., Phys. Rev. Lett. 77 (1996). Bratko, D., Chakraborty, A.K. and Shakhnovich, E.I., "Recognition Between Random Heteropolymers and Multifunctional Disordered Surfaces Due to Statistical Pattern Matching: Implications for Viral Inhibition and Chromatography", in press (1997). Sigal, G., Mammen, M., Dahmann, G. and Whitesides, G.M., J. Am. Chem. Soc. 118 3789 (1996).

Johnson, R.D., Wang, Z.G. and Arnold, F.H., J. Phys. Chem. 100 5134 (1996).

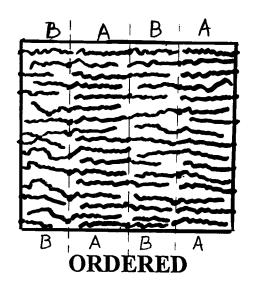
## **DISORDERED OR LAMELLAR STRUCTURE**



DISORDERED

 $\psi(\mathbf{r}) = 0$ 

 $LET \psi(r) = \Delta \cos Qr$ 



 $\psi(r) = PERIODIC$ **FUNCTION OF r** 

**Q = FREQUENCY** 

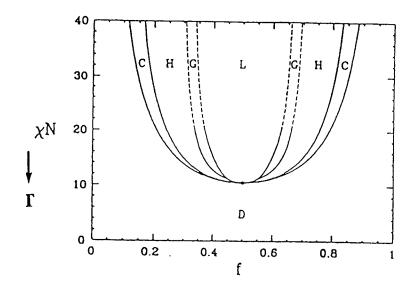
FOR THE DISORDERED STRUCTURE,  $\Delta = 0$ 

FOR THE LAMELLAR STRUCTURE,  $\Delta \neq 0$ 

**Q** IS A CHARACTERISTIC FREQUENCY CALCULATED FROM N, f,  $l_A$ ,  $l_B$  AND  $\chi$ 

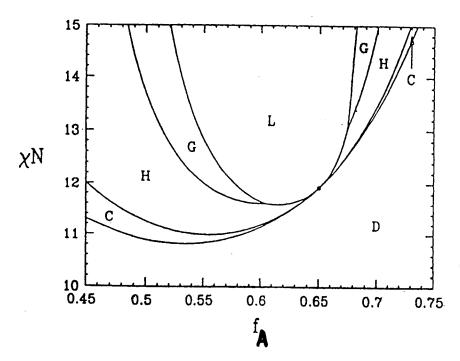
Q DETERMINES THE LAMELLAR THICKNESS.

# CALCULATED PHASE DIAGRAMS FOR A DIBLOCK COPOLYMER



# **SYMMETRIC CASE**

$$l_{\mathbf{A}} = l_{\mathbf{B}}$$
(LEIBLER, 1980)



# **ASYMMETRIC CASE**

$$\ell_{\mathbf{A}} = 3.16 \, \ell_{\mathbf{B}}$$

(MATSEN AND SCHIC 1994)

**C = BODY-CENTERED CUBIC** 

L = LAMELLAR

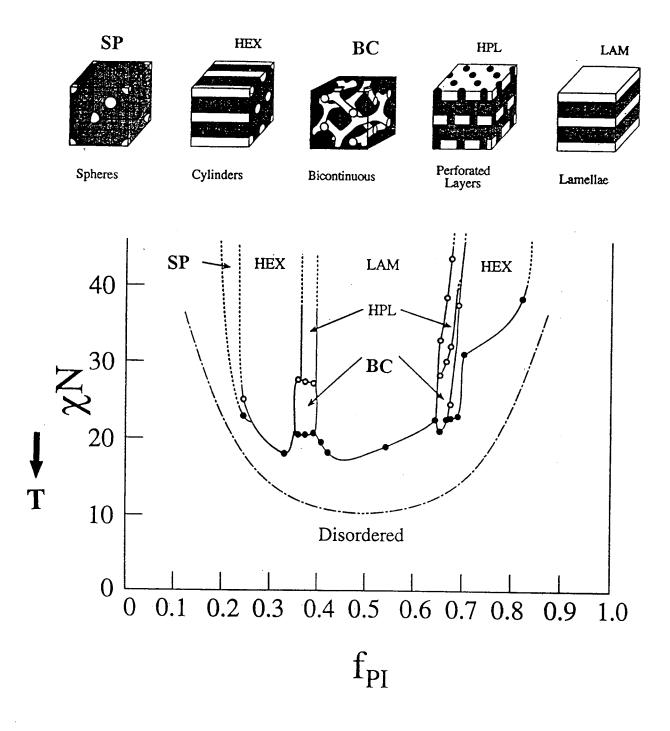
H = HEXAGONAL

**D** = **DISORDERED** 

G = GYROID

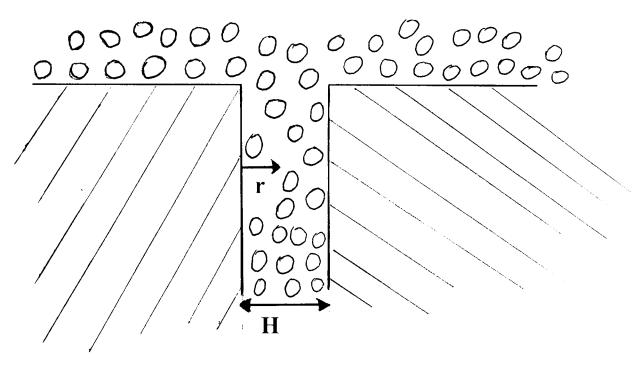
Figure 3

# EXPERIMENTAL RESULTS FOR DIBLOCK COPOLYMER POLYISOPRENE-POLYSTYRENE



(KHANDPUR ET AL, 1995)

# DENSITY-FUNCTIONAL THEORY APPLIED TOWARD CALCULATING PROPERTIES OF A CONFINED FLUID



FLUID IN PORE IS AT CONSTANT VOLUME, TEMPERATURE AND CHEMICAL POTENTIAL µ

μ (BULK) = μ (PORE) v(r) = POTENTIAL ACTING ON THE FLUID DUE TO THE WALL

H\* = REDUCED PORE DIAMETER

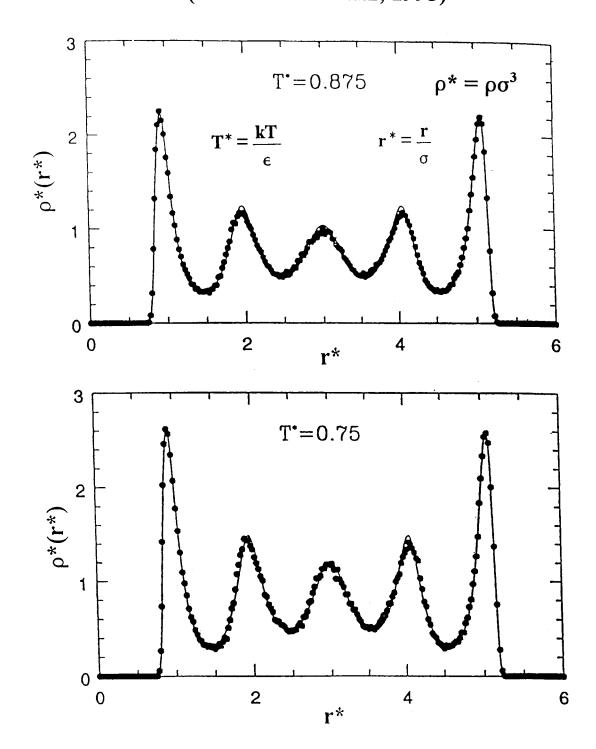
 $H^* = H/\sigma$ 

 $\sigma = MOLECULAR$  DIAMETER

GIVEN THE PROPERTIES OF THE BULK FLUID AND v(r), WHAT ARE THE PROPERTIES OF THE FLUID IN THE PORE?

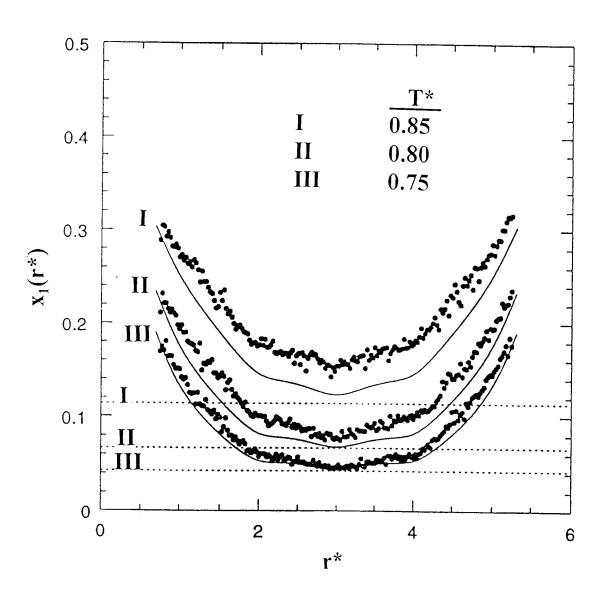
Figure 5

# DENSITY PROFILES IN A PORE WITH H\* = 6 (KIERLIK ET AL, 1995)



— DENSITY-FUNCTIONAL THEORY; ····· MONTE-CARLO SIMULATION

# COMPOSITION PROFILE IN PORE WITH $H^* = 6$ (KIERLIK ET AL, 1995)



 $x_1 = MOLE FRACTION OF COMPONENT 1$ 

····· = BULK COMPOSITION

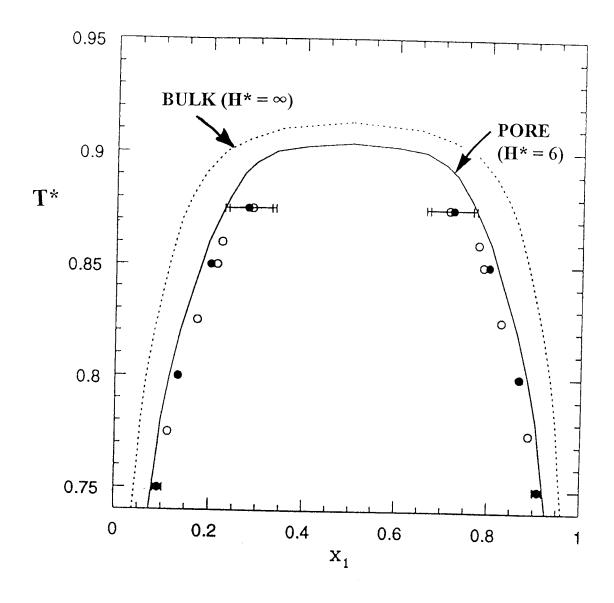
•••• = MONTE-CARLO SIMULATION

---- = DENSITY-FUNCTIONAL THEORY

Figure 7

# COEXISTENCE CURVE FOR A BINARY MIXTURE IN AN (ATTRACTIVE) PORE

# (KIERLIK ET AL, 1995)

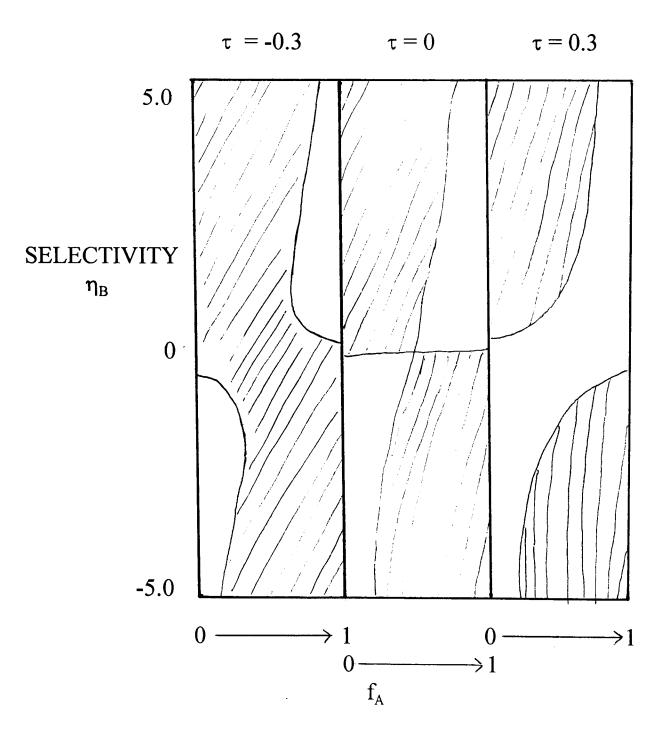


DENSITY-FUNCTIONAL THEORY

•, • MONTE-CARLO SIMULATIONS

## ADSORPTION-DEPLETION EQUILIBRIA FOR A TOTALLY RANDOM ( $\lambda = 0$ ) COPOLYMER (A, B) ON A HOMOGENEOUS SURFACE

(GUTMAN AND CHAKRABORTY, 1996)



SHADED AREAS SHOW ADSORPTION. OPEN AREAS SHOW DEPLETION.

# ADSORPTION OF AN (A-B) COPOLYMER ON A HETEROGENEOUS (● ○) SURFACE

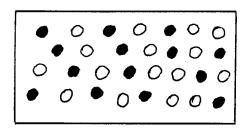


### PERFECTLY ALTERNATING COPOLYMER $\lambda = -1$



**BLOCKY COPOLYMER** 

 $1 > \lambda > 0$ 

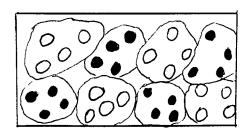


STRIATED SURFACE.

SITES • AND • HAVE A

"CHESSBOARD-LIKE"

DISTRIBUTION

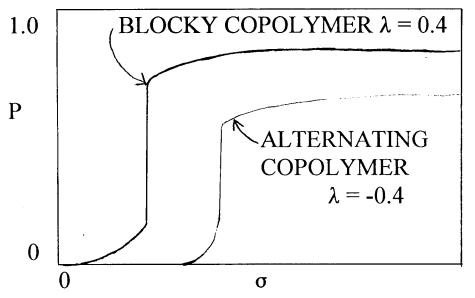


PATCHY SURFACE.

SITES ● AND ○ HAVE A

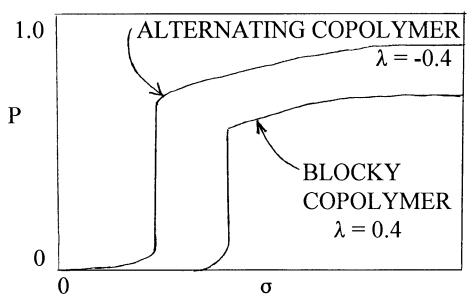
"PANCAKE" DISTRIBUTION

# RECOGNITION: ADSORPTION OF COPOLYMER ON A HETEROGENEOUS SURFACE DEPENDS ON STATISTICS OF DISTRIBUTION OF BOTH (FROM CHAKRABORTY et al)



STATISTICALLY
PATCHY
SURFACE

σ IS THE DENSITY OF SURFACE SITES (TOTAL NO. OF SITES PER UNIT AREA)



STATISTICALLY
STRIATED
SURFACE

P = FRACTION OF ALL POLYMER SEGMENTS THAT ARE ADSORBED

P = 0, NO ADSORPTION

P = 1, TOTAL ADSORPTION